ORGANIC LETTERS

2009
Vol. 11, No. 24
5686−5689

Oxygen- and Sulfur-Containing Positively Charged Polycyclic Aromatic Hydrocarbons

Dongqing Wu, Wojciech Pisula,[†] Monika C. Haberecht,[§] Xinliang Feng,* and Klaus Müllen*

Max Planck Institute for Polymer Research, Ackermannweg 10, D-55128, Mainz, Germany

feng@mpip-mainz.mpg.de; muellen@mpip-mainz.mpg.de

Received October 19, 2009

ABSTRACT

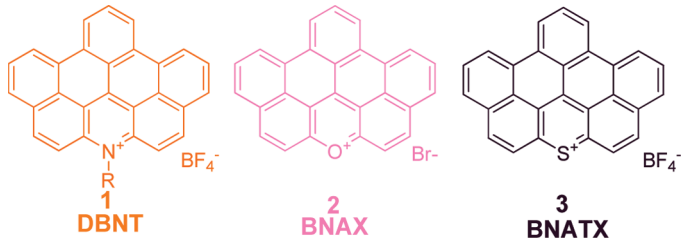

Benzo[5,6]naphthaceno[1,12,11,10-*jklmna*]xanthylium (BNAX) and benzo[5,6]naphthaceno[1,12,11,10-*jklmna*]thioxanthylium (BNATX) salts were synthesized. Comparison of the UV−vis absorption and emission spectra of them and dibenzo[*jk,mn*]naphtho[2,1,8-*fgh*]thebenidinium (DBNT) salts suggests that the incorporation of different heteroatoms in the same PAH core changes their optoelectronic properties profoundly. Ordered columnar liquid crystalline phases were observed for di- and tridodecyl-substituted BNAX salts. X-ray scattering and molecular modeling indicate that three BNAX molecules self-assemble into a disklike structure, which further organizes into hexagonal columnar phases.

Large polycyclic aromatic hydrocarbons (PAHs), as subunits of graphene, have been exploited in various organic electronic devices including field-effect transistors, injection layers, and solar cells.[1] Compared with their all-hydrocarbon analogues, PAHs containing heteroatoms such as nitrogen in the aromatic framework, either neutral or positively charged, exhibit unprecedented chemical and physical properties.[2]

Very recently, we described the synthesis and self-assembly of dibenzo[*jk,mn*]naphtho[2,1,8-*fgh*]thebenidinium (DBNT, **1**, Figure 1) salts,[3] which were the largest nitrogen-containing positively charged PAHs. Compared with the well-studied DBNT salts,[3,4] their analogues containing other heteroatoms such as sulfur and oxygen have been relatively unexplored. In this paper, we present the first examples of oxygen- and sulfur-containing positively charged PAHs, namely benzo[5,6]naphthaceno[1,12,11,10-*jklmna*]xanthylium (BNAX, **2**) and benzo[5,6]naphthaceno[1,12,11,10-*jklmna*]thioxanthylium (BNATX, **3**) salts (Figure 1). Following the order of nitrogen, oxygen, and sulfur, these three types of positively charged PAHs show obvious bathochromic shifts of their UV−vis absorption and emission bands,

[†] Present address: Evonik Degussa GmbH, Process Technology & Engineering, Process Technology - New Processes, Rodenbacher Chaussee 4, D-63457, Hanau-Wolfgang, Germany.

[§] Present address: BASF SE, Polymer Research, Carl-Bosch-Str. 38, D-67056, Ludwigshafen, Germany.

(1) (a) Hoeben, F. J. M.; Jonkheijm, P.; Meijer, E. W.; Schenning, A. *Chem. Rev.* **2005**, *105*, 1491. (b) Wu, J. S.; Pisula, W.; Müllen, K. *Chem. Rev.* **2007**, *107*, 718.

(2) (a) Pieterse, K.; van Hal, P. A.; Kleppinger, R.; Vekemans, J.; Janssen, R. A. J.; Meijer, E. W. *Chem. Mater.* **2001**, *13*, 2675. (b) Draper, S. M.; Gregg, D. J.; Madathil, R. *J. Am. Chem. Soc.* **2002**, *124*, 3486. (c) Wu, D. Q.; Zhi, L. J.; Bodwell, G. J.; Cui, G. L.; Tsao, N.; Müllen, K. *Angew. Chem., Int. Ed.* **2007**, *46*, 5417. (d) Takase, M.; Enkelmann, V.; Sebastiani, D.; Baumgarten, M.; Müllen, K. *Angew. Chem., Int. Ed.* **2007**, *46*, 5524. (e) Bunz, U. H. F. *Chem.—Eur. J.* **2009**, *15*, 6780. (f) Miao, S.; Appleton, A. L.; Berger, N.; Barlow, S.; Marder, S. R.; Hardcastle, K. I.; Bunz, U. H. F. *Chem.—Eur. J.* **2009**, *15*, 4990.

(3) Wu, D. Q.; Feng, X. L.; Takase, M.; Haberecht, M. C.; Müllen, K. *Tetrahedron* **2008**, *64*, 11379.

(4) Benniston, A. C.; Rewinska, D. B. *Org. Biomol. Chem.* **2006**, *4*, 3886.

10.1021/ol902366y
Published on Web 11/17/2009

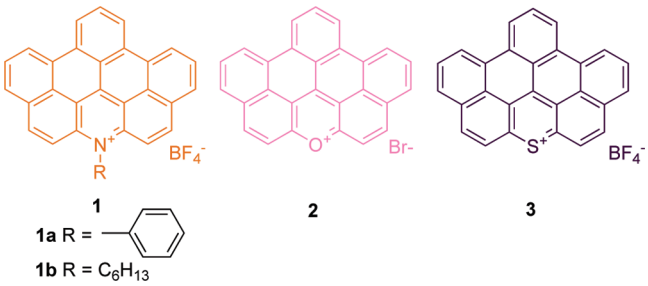

Figure 1. DBNT (**1**), BNAX (**2**), and BNATX (**3**) salts.

indicating that heteroatoms can effectively adjust the photophysical properties of PAHs without alteration of the aromatic skeleton. The bulk organization of alkyl-chain-substituted BNAX is also presented. Both di- (**2c**) and tridodecyl-substituted (**2d**) BNAX salts can form columnar liquid crystalline phases with large unit cells. This can be attributed to the formation of disklike substructures by the self-assembly of three BNAX molecules.

The synthesis of various BNAX bromides (**2**) proceeds as follows (Scheme 1): a Claisen condensation of appropriate arylaldehydes and naphthols in acetic acid results in 14-phenyl-14*H*-dibenzo[*a,j*]xanthenes **4a**−**d**.[5] Mono- (**4b**), di- (**4c**), and tribromodibenzo[*a,j*]xanthene (**4d**) constitute useful building blocks for the synthesis of functionalized BNAX salts. In our work, the Kumada coupling of **4b**−**d** with Grignard reagents produces the alkyl-substituted dibenzo[*a,j*]xanthenes (**4e**−**g**) in good yields. Subsequent oxidization of **4** with bromine yields the corresponding 14-phenyl-14-dibenzo[*a,j*]xanthenylium bromides (**5a**−**d**). The photocyclization of **5** in acetic acid under 300 nm UV light results in BNAX bromides **2** as purple solids without the need for further purification. All molecules were characterized by $^{1}H/^{13}C$ NMR spectroscopy, FD/MALDI-TOF mass spectrometr,y as well as elemental analysis (Supporting Information).

Scheme 1. Synthesis of BNAX Bromides

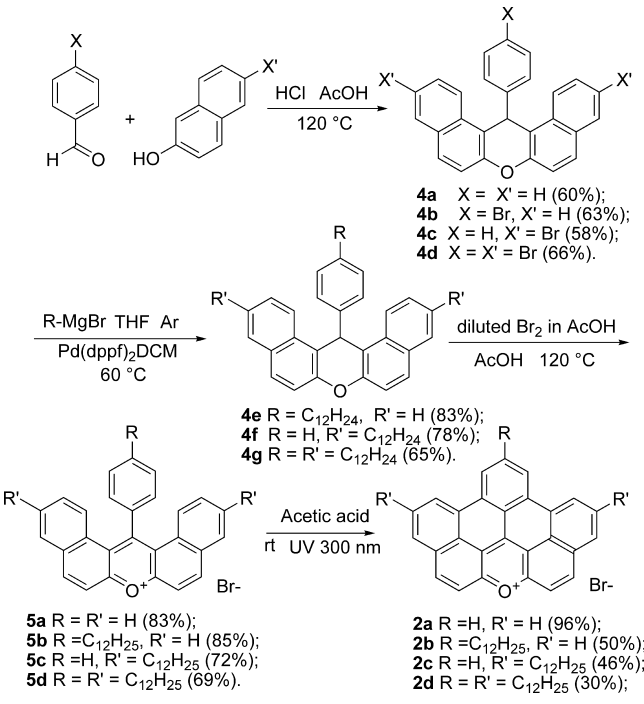

For the synthesis of the sulfur-containing BNATX salt, a modified synthetic route was developed in this work (Scheme 2): the acid-catalyzed ether−sulfide exchange reaction[6] between 2-methoxynaphthalene and naphthalene-2-thiol gives dinaphthalen-2-ylsulfane (**6**), which can further condense with benzaldehyde to provide 14-phenyl-14*H*-dibenzo[*a,j*]thioxanthene (**7**).[7] Then, 14-phenyldibenzo[*a,j*]thioxanthenium tetrafluoroborate (**9**) is obtained based on a two-step procedure through the oxidization of **7** and subsequent dehydrogenation of the resulting 14-phenyl-14*H*-dibenzo[*a,j*]thioxanthen-14-ol (**8**). Since compound **7** cannot be directly oxidized with bromine as in the case of **4**, we utilize a two-step oxidization−dehydration process. Irradiation of **9** with 300 nm UV light yields benzo[5,6]naphthaceno[1,12,11,10-*jklmna*]thioxanthylium tetrafluoroborate (BNATX BF_4, **3**) as purple needles.

Scheme 2. Synthesis of BNTAX Salt

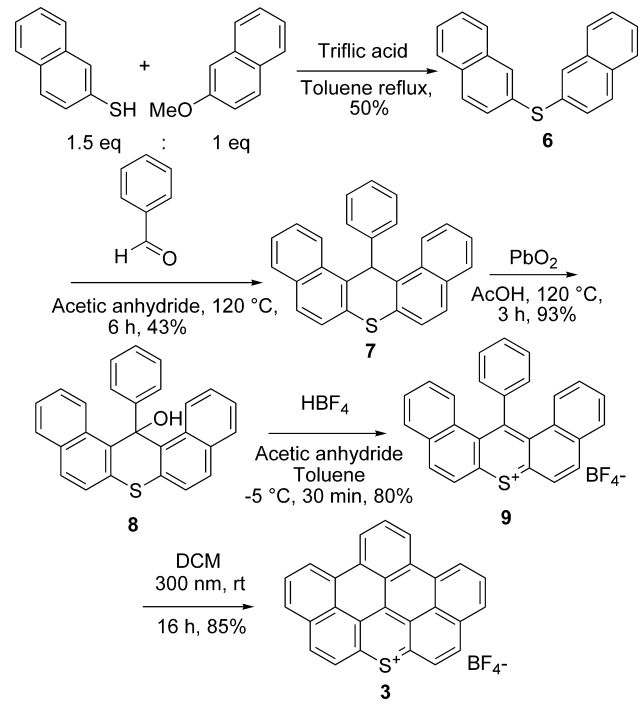

(5) (a) Claisen, L. *Ber. Deutsch. Chem. Ges.* **1887**, *20*, 665. (b) Claisen, L.; Claparede, A. *Ber. Deutsch. Chem. Ges.* **1887**, *14*, 2460.

(6) Radhakrishnan, K.; Lin, C. H. *Synlett* **2005**, 2179.

(7) (a) Dilthey, W.; Quint, F.; Heinen, J. *J. Prakt. Chem.* **1939**, *152*, 49. (b) Dilthey, W.; Quint, F.; Stephan, H. *J. Prakt. Chem.* **1939**, *152*, 99.

Further characterization of the product by FD/MALDI-TOF mass spectrometry, $^{1}H/^{13}C$ NMR spectroscopy, and elemental analysis is in accordance with expectations (Supporting Information).

In order to understand the effect of different heteroatoms on the optoelectronic properties of charged PAHs with the same aromatic framework, the UV−vis absorption spectra of 14-phenyl-DBNT tetrafluoroborate **1a**, BNAX bromide **2a**, and BNATX tetrafluoroborate **3** in dichloromethane solutions are compared in Figure 2a. Remarkably, the three

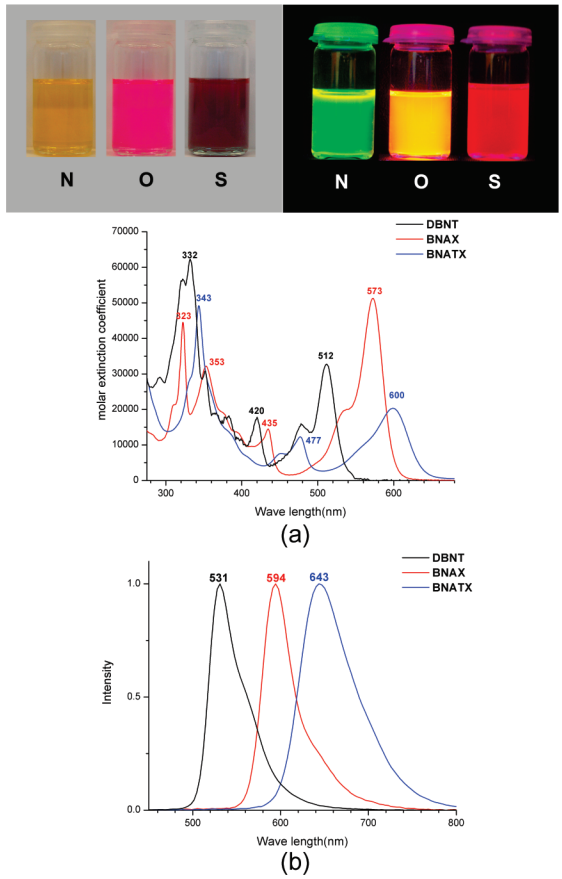

Figure 2. (a) UV−vis absorption spectra of **1a** (black), **2a** (red), and **3** (blue) in CH_2Cl_2, measured at 20 °C. (b) Fluorescence spectra of **1a** (black), **2a** (red), and **3** (blue) in dichloromethane (20 °C, excited at 350 nm).

compounds show very different absorption spectra, especially in the visible region. The maximum absorptions for **1a**, **2a**, and **3** are located at 512 (log $\varepsilon = 4.51$), 573 (log $\varepsilon = 4.71$), and 600 nm (log $\varepsilon = 4.31$), respectively, thus reflecting an apparent red shift by 61 (N to O) and 27 nm (O to S). The emission spectra are recorded by using the same excitation wavelength of 350 nm for **1a**, **2a** and **3**; the results are demonstrated in Figure 2b. The three spectra show structureless peaks which are centered at 531, 593, and 643 nm, respectively. Obviously, this red-shift trend following the sequence of nitrogen, oxygen, and sulfur is consistent with their maximum absorptions in the visible region. Similar phenomena have been recognized in the study of small heterocations such as pyridinium, pyrylium, and thiopyrylium salts.[8] Our results, therefore, demonstrate the possibility of fine-tuning the optoelectronic properties of PAHs through the incorporation of different heteroatoms without changing the aromatic framework.

The supramolecular chemistry of alkyl-substituted BNAX salts was also studied in this work. Scanning electron microscopy images of compound **2b** (7-dodecylbenzo-[5,6]naphthaceno[1,12,11,10-*jklmna*]xanthylium bromide) drop-cast from a methanol solution exhibit fibrous aggregates (Figure S3, Supporting Information) close to the nanofibers formed from 14-hexyl-DBNT tetrafluoroborate **1b**.[3] This suggests a similar self-assembly mechanism in methanol. On the other hand, the supramolecular organization of positively charged PAHs substituted with more than one alkyl chain in the bulk is still unknown. Thus, the liquid crystalline properties of the di- (**2c**, 4,10-didodecylbenzo[5,6]naphthaceno[1,12,11,10-*jklmna*]xanthylium bromide)- and tridodecyl (**2d**, 4,7,10-tridodecylbenzo[5,6]-naphthaceno[1,12,11,10-*jklmna*]xanthylium bromide)-substituted BNAX bromides were investigated by two-dimensional wide-angle X-ray scattering (2D-WAXS). For this purpose, extruded filaments with macroscopically aligned columnar structures were prepared from both compounds at 120 °C. Neither compound reveals any phase transition in differential scanning calorimetry (DSC) scans within a temperature range of −100 to +300 °C. The 2D patterns shown in Figure 3 are

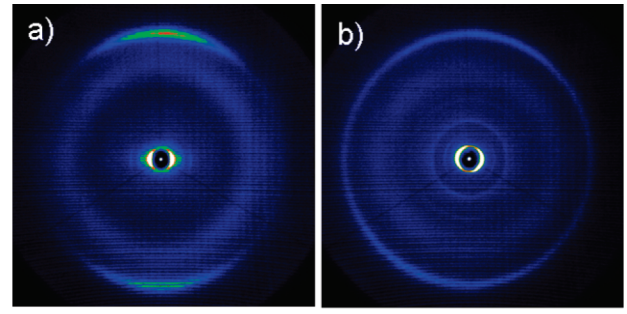

Figure 3. 2D-WAXS patterns of (a) **2d** and (b) **2c** both recorded at 30 °C.

similar for both compounds indicating identical supramolecular structures. The distribution of the reflections in the pattern is characteristic for a discotic liquid crystalline phase and can be separated into an equatorial and meridional plane. The equatorial small angle reflections are assigned to typical columnar stacks formed from the discotic molecules. Identical to most discotics the columns are well-aligned in the orientation of the extruded fiber direction. The positions of the reflections are thereby related to a unit cell characteristic for the intercolumnar arrangement. In this case, a hexagonal cell with a parameter of

(8) (a) Saeva, F. D.; Olin, G. R. *J. Am. Chem. Soc.* **1980**, *102*, 299. (b) Novikov, V. N.; Tymyanskii, Y. R.; Feigelman, V. M.; Knyazhanskii, M. I. *Khim. Geterotsikl. Soedin.* **1988**, 1320. (c) Beddoes, R.; Heyes, D.; Menon, R. S.; Watt, C. I. F. *J. Chem. Soc., Perkin Trans. 2.* **1996**, 307.

3.97 nm for **2d** is derived, while for **2c** a slightly smaller parameter of 3.49 nm is determined.

The wide angle meridional reflections in both patterns of **2d** and **2c** are attributed to a π-stacking distance of 0.34 nm between aromatic cores within the columnar structures. The molecules are packed in a nontilted manner with their planes perpendicular to the columnar axis. The structural analysis suggests that **2d** forms a columnar liquid crystalline phase due to the typical hexagonal unit cell, nontilted stacked disks, and finally the appearance of an amorphous halo, which is attributed to the disordered alkyl chains (Figure S4, Supporting Information). Interestingly, the organization and the corresponding dimensions of the liquid crystalline phase do not change at higher temperatures (Figure S5, Supporting Information, 150 °C) suggesting a pronounced stability of this thermal state.

The main difference between **2c** and **2d** is obvious from the meridional reflections owing to π-stacking correlations. Since **2d** is more waxy, the compound is therefore better macroscopically aligned, leading to reflections with a smaller azimuthal distribution. On the other hand, the sharp but rather isotropic scattering intensities for **2c** can be attributed to poorer orientation of the powder-like sample.

It is interesting that the parameters of the unit cell for both compounds are almost two times larger than the simple molecular size (the fully stretched lengths of **2c** and **2d** are 2.0 and 2.2 nm, respectively.[9]), which is very similar to what we have observed in other discotic liquid crystal materials consisting of positively charged PAHs.[10] It is reasonable to assume that a kind of oligomer structure is first formed in the liquid crystal phase of **2c** and **2d** due to noncovalent forces between the molecules, including dipole−dipole, ionic, and amphiphilic interactions. These oligomeric discs then form discotic columnar stacks by the local phase separation between their soft and rigid parts.[11] According to the parameters obtained by WAXS, the effective number of molecules **Z** per repeat distance (or slice) for **2c** and **2d** is determined as 2.97 and 2.90 at 30 °C (Supporting Information).[12] Therefore, a molecular model for the columnar liquid crystal of **2d** is illustrated in Figure 4. In this model, three BNAX salts self-assemble into a disklike trimer. These trimers then form columnar superstructures which further arrange into the hexagonal columnar mesophases. The dimension of the disklike trimer is in good agreement with the dimension of **2d** in this model. The molecular packing of **2c** in the bulk is similar.

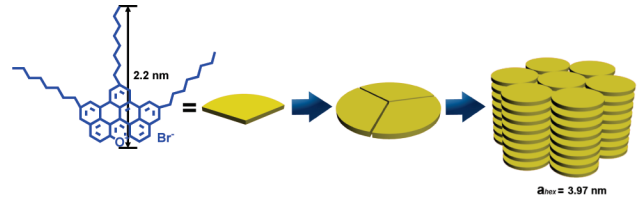

Figure 4. Scheme illustration of the unit cell formed by **2d**.

In this work, the synthesis of a class of unprecedented large oxygen- and sulfur-containing positively charged BNAX and BNATX salts was developed. These molecules exhibited interesting optoelectronic properties which strongly depend on the heteroatoms in their aromatic framework. Columnar liquid crystals were formed by the trimers of alkyl-chains-substituted BNAX salts due to noncovalent intermolecular forces. Combined with our previous results,[3] extending the synthetic methodology to even larger positively charged PAHs with different heteroatoms is currently underway in our laboratory. Physical studies of these compounds as well as our exploration of their applications are also in progress.

Acknowledgment. This work was financially supported by the Max Planck Society through the program ENERCHEM, the German Science Foundation (Korean-German IRTG), DFG Priority Program SPP 1355, and DFG Grant No. AN 680/1-1.

Supporting Information Available: Experimental details and characterization data of all new compounds. This material is available free of charge via the Internet at http://pubs.acs.org.

OL902366Y

(9) The MM2 force field was used to calculate the minimum energy conformation during computer simulations.

(10) Wu, D. Q.; Pisula, W.; Enkelmann, V.; Feng, X. L.; Müllen, K. *J. Am. Chem. Soc.* **2009**, *131*, 9620.

(11) Sergeyev, S.; Pisula, W.; Geerts, Y. H. *Chem. Soc. Rev.* **2007**, *36*, 1902.

(12) Lava, K.; Binnemans, K.; Cardinaels, T. *J. Phys. Chem. B* **2009**, *113*, 9506.